Express Polymer Letters Vol.19, No.11 (2025) 1133–1143
Available online at www.expresspolymlett.com
https://doi.org/10.3144/expresspolymlett.2025.83

Research article

Basalt fibers as a sustainable alternative to glass fibers in the reinforcement of polyamide 6 for gear applications

Rebeka Lorber[1], *József Gábor Kovács*[2], *Andreas Hausberger*[3], *Polona Umek*[4], *Miroslav Huskić*[1,5,6*], *Aleš Hančič*[5]

[1]Faculty of Polymer Technology, Ozare 19, 2380 Slovenj Gradec, Slovenia
[2]Budapest University of Technology and Economics, Faculty of Mechanical Engineering, Department of Polymer Engineering, Műegyetem rkp. 3, 1111 Budapest, Hungary
[3]Polymer Competence Center Leoben GmbH, Roseggerstraße 12, A-8700 Leoben, Austria
[4]Jožef Stefan Institute, Solid State Physics Departmen, Jamova cesta 39, 1000 Ljubljana, Slovenia
[5]TECOS, Slovenian Tool and Die Development Centre, Kidričeva 25, 3000 Celje, Slovenia
[6]Pomurje Science and Inovation Centre, ZIS Pomurje, Lendavska ulica 5a, 9000 Murska Sobota, Slovenia

Received 18 June 2025; accepted in revised form 31 July 2025

Abstract. With the increasing use of e-mobility, the demand for high-quality materials to produce polymer gears is growing. Due to the tendency towards using natural materials and reducing carbon footprint, basalt fibers (BF) are tested as a substitute for glass fibers (GF). For this purpose, composites of polyamide 6 (PA6) with GF and BF, with and without compatibilizer and polytetrafluoroethylene (PTFE) are produced, tested, and properties compared. The mechanical, thermomechanical, thermal, and tribological properties of the composites, as well as the size of the fibers after the production of the composites and after injection molding, are determined. The compatibilizer improves the impact strength, while the glass fibers have a better reinforcing effect. The fibers increase crystallinity, but the effect is minimal. The thermal conductivity increases approximately the same for both fibers and is highest at composites that, in addition to 30% fibers, also contain PTFE. The tribological properties are comparable but slightly better for glass fibers. The fiber length is greatly reduced during the production of the composites and is around 200–300 μm in both cases. SEM imaging and mapping analysis show good dispersion of the fibers in the polymer and relatively poor compatibility with PA6.

Keywords: *thermoplastic composites, glass fibres, mechanical properties, short-fibre composites, natural fibre composites, structural composites, tribological properties*

1. Introduction

Fiber-reinforced plastic composites (FRPC) have been used for decades in the marine, automotive, aerospace, electronic, sports, and other industrial sectors. Currently, glass fiber-reinforced plastics (GFRP) account for over 90% of the FRPC. Consumption of carbon fibers is far in second place, while consumption of other reinforcing fibers is negligible.

However, the interest in basalt fibers (BF) to produce reinforced plastic composites (BFRPC) is increasing, especially in the scientific community. One-half of the articles about BFRPC have been published within the last three years (2021–2024, Web of Science). There are various reasons for this high interest in BF. They seem to be a sustainable alternative to glass fibres (GF) and especially carbon fibers due to low energy consumption, smaller CO_2 footprint, and absence of various additives, especially boron-based, during production [1]. BF is also known for high levels of eco-compatibility and recyclability, resulting in a high-performance green inorganic material. The

*Corresponding author, e-mail: miroslav.huskic@zis.si

acid resistance of BF is greater than that of glass fibers, and the alkali resistance is similar. Mechanical properties are better than E-glass fibers; however, they are not as good as S-glass or carbon fiber [2–5]. Although BF is chemically very similar to asbestos fibers, it is not toxic or carcinogenic [6, 7]. All those benefits and the lower cost of BF are probably the most important factors for increased interest and use of BF.

BF can be obtained in the form of short or continuous fibers or fabrics. The quality and mechanical properties of short fibers might be inferior to long ones due to different methods of preparation [4]. Besides, BF is sensitive to humidity and water, which changes both surface chemistry and morphology [8, 9]. However, surface modification can improve resistance to environmental aging as well as the mechanical properties of polymer composites [2, 5, 10, 11].

Many polymer composites with basalt fibers, both thermoplastics and thermosets, have already been produced, and some good review articles have recently been published on this topic [2, 11, 12]. Thermosets are usually made with long fibers or fabrics, while thermoplastic composites are mostly made with short or chopped BF.

Although BF is intended as a substitute for GF, there are not many studies comparing the properties of BF and GF polymer composites. Most of them are comparing thermosetting composites. Epoxy laminates with BF showed better mechanical properties than the laminates based on E-glass fibers [13, 14]. Tensile strength values of BF composites were close to those of carbon fiber laminates, and the behavior under fatigue conditions indicated superior performances of BF laminates to the GF laminates, with an improved capability of sustaining progressive damage and slightly higher damping properties [13]. However, epoxy sheet molding compounds, which were prepared with short fibers, showed only slightly better mechanical properties, and in both samples, the primary failure mechanism was fiber pull-out due to interfacial debonding [15]. A comparison of the tensile and shear behavior for basalt and glass epoxy composites at different strain rates showed that although the tensile properties of BF/epoxy were better, the shear modulus and strength were much lower. This was attributed to a weak interfacial adhesion of epoxy to BF compared to GF [16]. BF and E-glass woven fabric–reinforced vinyl-ester composites have also been compared. BF/vinyl-ester composite showed higher interlaminar shear strength and flexural modulus than the E-glass/vinyl ester but lower flexural strength [17]

One of the important application fields where BF could enter and substitute GF is plastic gears. There is an increased need for better quality and more durable gears, especially for electric bikes and scooters. Materials for gears should not only have good mechanical properties but also better tribological behavior, which is usually obtained by the addition of polytetrafluoroethylene (PTFE). The goal of this research was to evaluate BF as a substitute for GF in gear production. Composites based on PA6 with BF or GF, with and without PTFE, were prepared, and their mechanical, thermal, and tribological properties were compared.

2. Experimental

2.1. Materials

PA6 was Akulon K222-D, produced by DSM, Emmen, Netherlands. PA6-based compounds were stabilized using antioxidant AT 10, which was purchased from AMIK ITALIA S.p.a, Milano, Italy. To improve the adhesion of the components, a commercially available adhesion promoter, Fusabond N416 (DuPont, Wilmington, Delaware, USA), was used, which is a maleic anhydride grafted ethylene elastomer with an MFI of 23 g/10 min.

PA6 was reinforced using either Basaltex Basalt fibers (Technobasalt, Slavuta city, Ukraine), RBR-18-T5/5 with a diameter of 17±1 μm and 5 mm chop length, or glass fibers DS1128-10N (Braj Binani Group, Mumbai, India) with a diameter of 10 μm and 4 mm chop length.

To improve the tribological properties of compounds, PTFE powder Fluon FL 1690 (AGC Chemicals Europe, Thornton-Cleveleys, UK), with a bulk density of 44 g/L, mean particle size of 40 μm, and surface area of 1.8 m^2/g, was added to selected compounds.

2.2. Sample preparation

Six composites and one polymer blend based on PA6 were compounded, and the properties were compared to pure PA6. The composites were reinforced with either 30% GF or BF, with and without compatibilizer (3%), and with or without internal lubricant (15% PTFE). The antioxidant in the quantity of 0.5% was added in all cases. The selected quantities are based on the most common practice in the

Table 1. Sample designations and composition.

Sample	PA6 [%]	Fiber	Compatibiliser [%]	PTFE	Antioxidant [%]
PA6	99.5	/	/	/	0.5
PA6-C	96.5	/	3	/	0.5
PA6BF	69.5	BF, 30%	/	/	0.5
PA6BF-C	66.5	BF, 30%	3	/	0.5
PA6BF-C-PTFE	51.5	BF, 30%	3	15	0.5
PA6GF	69.5	GF, 30%	/	/	0.5
PA6GF-C	66.5	GF, 30%	3	/	0.5
PA6GF-C-PTFE	51.5	GF, 30%	3	15	0.5

production of gear material. The sample designations and compositions are presented in Table 1.

Compounding was performed on a corotating twin-screw extruder Labtech LTE 26-44 (Labtech Engineering Co., Ltd., Samut Prakan, Thailand) with a screw diameter of 26 mm, at a screw speed of 80 rpm. The filament was air-cooled before being granulated using a Labtech LZ-120/VS granulator. The temperature profile for extrusion was increasing from 160 °C at the dosing to 245 °C at the die.

The prepared composites were injection molded into test specimens according to standards ISO 527 (type 1BA), ISO 178, and ISO 179 using a Krauss-Maffei CX50-180 injection molding machine with 50 t clamping force and a screw diameter of 30 mm (Krauss-Maffei, Parsdorf, Germany). The melt temperature was 230 °C, the mold temperature was 80 °C, the screw speed was 30 rpm, the injection speed was 50 mm/s, and the cooling time was 20 s.

2.3. Characterisation

Mechanical properties were determined by tensile, flexural, and impact tests, according to the above-mentioned standards. Five specimens were tested. Tensile and flexural tests were performed using Shimadzu AG-X plus, equipped with a 10 kN load cell and an optical extensometer Shimadzu TRViewX (Shimadzu, Kyoto, Japan). Impact tests were conducted using a pendulum impact tester LIYI LY-XJJD5 (Liyi Environmental Technology Co., Dongguan, China), with a pendulum impact velocity of 2.9 m/s. Impact toughness and notched impact toughness were tested using the energies of 5 and 2 J, respectively.

Dynamic mechanical analysis was performed employing Perkin Elmer DMA 8000 (Perkin Elmer Inc., Waltham, Massachusetts, USA) at a frequency of 1 Hz with an amplitude of 0.005 mm from 25 to 200 °C with a heating rate of 2 °C/min. One measurement was performed for each sample.

Thermal properties were determined by dynamic scanning calorimetry (DSC). Samples were heated/cooled twice, with the heating/cooling rate of 10 K/min in a nitrogen atmosphere (20 mL/min) using a Mettler Toledo DSC 2 calorimeter (Mettler-Toledo, Greifensee, Switzerland). The temperature range was 0 to 260 °C. Two measurements were performed for each sample.

The results of the second heating were used for the determination of the degree of crystallinity. The degree of crystallinity (X_c [%]) was determined using Equation (1), where the H_f of PA6 was 230 J/g :

$$X_c = \frac{H_m}{H_f} \cdot 100 \quad (1)$$

Thermal conductivity was determined by the hotdisk method, using HotDisk TPS1500 (Hot Disk AB, Gothenburg, Sweden). Measurements were performed according to ISO 22007-2 standard using a Kapton sensor with a 3.189 mm radius. The surrounding temperature was 25 °C.

Tribological properties were studied employing the pin-on-disc method. Tests were conducted according to the ASTM G99 standard on the tribometer Bruker UMT-2 (Bruker Corporation, Billerica, Massachusetts, USA). The applied load was 1 MPa, velocity 1 m/s, and test duration 4 h. Polymeric pins were machined out of the injection molded tensile test bars (shoulder region, opposite of the injection point) with a cross-sectional area of 4×4 mm using a CNC milling machine with an average surface roughness of R_a 0.8 µm. The used counterbodies were made of 34CrNiMo6 steel with an average surface roughness R_a of 0.3 µm. For all tests, at least two repetitions were conducted. The calculation of the coefficient of friction (CoF) (friction force in relation to the

normal force) was carried out in the steady state region after the running-in phase of the test. The wear rate (K) was calculated considering the volumetric mass loss (mass loss/density) in relation to the applied load. After each tribological test, failure analysis was performed using Zeiss Axioscope7 and Zeiss Stemi 2000C microscopes and different magnifications (8×, 25×, 50×, and 100×) (Zeiss, Oberkochen, Baden-Württemberg, Germany).

For the microscopic examination of the glass fibers, samples were prepared by burning out the matrix material at 550 °C for 3 h in a Denkal 6B annealing furnace. The fiber lengths were measured using a Keyence VHX-5000 optical microscope (Keyence Corporation, Osaka, Japan). Before capturing the microscopic images and analyzing the fibers, the glass fibers were evenly distributed on a glass plate. The length of approximately 1000 randomly selected glass fibers was measured.

The texture of the fracture surface of the samples and the distribution of fillers within the polymer matrix were characterized using a scanning electron microscope (SEM), Quanta 650 v14 (Thermo Fischer, Waltham, Massachusetts, USA). For SEM preparation, a piece of a polymer composite was attached to an aluminum stub using thin, conductive double-sided carbon tape. Immediately before the SEM investigation and energy dispersive X-ray spectroscopy (EDXS) analysis, a 5 nm thick Au/Pd layer was deposited on the specimen to reduce the charging effect.

3. Results and discussion

3.1. Mechanical properties

The results of the tensile and flexural moduli of all materials are shown in Figure 1. The addition of an elastomeric compatibilizer to PA6 reduced tensile and flexural modulus by approximately 50% (from 1.65 to 0.82 GPa) and 40% (from 1.9 to 1.14 GPa), respectively. The addition of fibers to PA6 greatly increased both moduli. However, the addition of fibers increased tensile moduli more than the flexural one. The addition of BF and GF increased tensile modulus to 4.46 and 6.55 GPa, respectively, while flexural modulus increased to 4.34 and 5.06 GPa, respectively.

The addition of a compatibilizer to composites only slightly reduced the flexural moduli, but a significant reduction was observed in tensile moduli for both composites. The value decreased from 4.46 to 3.44 GPa (23%) and from 6.55 to 5.99 GPa (9%) for BF and GF composites, respectively.

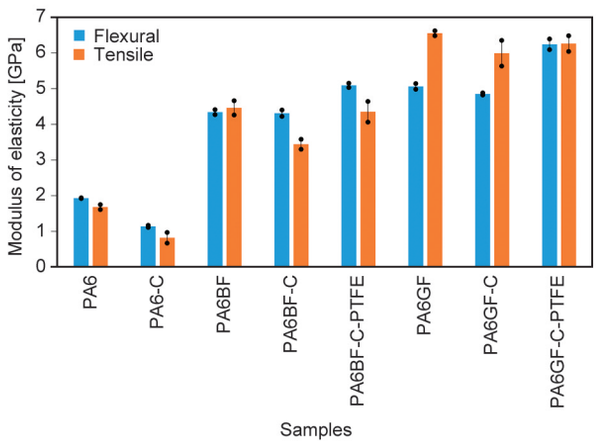

Figure 1. Tensile and flexural moduli of materials.

The addition of PTFE particles increased both the tensile and flexural moduli. The tensile modulus of the BF composite reached 4.35 GPa, which is almost the same value as the non-compatibilized composite (4.46 GPa), while the flexural modulus reached 5.09 GPa. The tensile and flexural moduli of GF composites increased to 6.26 and 6.24 GPa, respectively. According to these results, much stiffer materials can be prepared by GF compared to BF, and the stiffness might be additionally increased by PTFE.

The results of the tensile and flexural strength (Figure 2) follow a similar trend as the moduli. The addition of compatibiliser reduced both strengths by approximately 50%. The tensile and flexural strength of PA6 were 57.2 and 79.3 GPa, respectively. After the addition of compatibilizer, they dropped to 29.4 GPa (tensile) and 44.4 GPa (flexural).

The addition of BF increased the strength of PA6 to 79.4 GPa (tensile) and 123.5 GPa (flexural). The addition of a compatibilizer decreased these values by approximately 10%, to 71.3 GPa (tensile) and

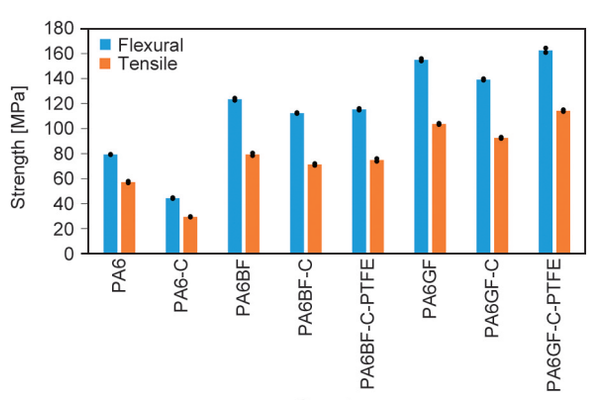

Figure 2. Tensile and flexural strength of materials.

112.4 GPa (flexural). The addition of PTFE increased both values again, but they remained lower than for non-compatibilized composites (74.9 GPa (tensile) and 115.4 GPa (flexural)). The increase of PA6 strength with the addition of PTFE particles is in agreement with previous findings [18].

The increase in strength was much larger when GF was added. The tensile strength increased to 103.7 GPa, while the flexural strength reached 155.1 GPa. Compared to BF these values are 31% and 26% higher. The addition of a compatibilizer slightly reduced both strengths. However, when PTFE was added the strongest composites were obtained. The tensile and flexural strengths were 114.3 and 162.6 GPa, respectively.

The impact toughness also seems to be better with GF than with BF. PA6 and PA6-C do not break if the samples are not notched. However, the notched impact strength of PA6 increased from 10.3 to 31.0 kJ/m^2 with the addition of only 3% of compatibilizer.

The addition of fibers reduced the impact strength of the polymer matrix and all the samples of all composites broke under the impact. However, the reduction was larger with BF (45–55 kJ/m^2) than GF (60–71 kJ/m^2). Notched impact strength, except for PA6BF (9.1 kJ/m^2), remained higher (13–18 kJ/m^2) than the strength of pure PA6 (10.3 kJ/m^2). The results are shown in Figure 3.

Viscoelastic properties of materials were determined because gears are dynamically loaded and the temperature may rise significantly during the operation. The results of storage moduli at 30 and 120 °C of all materials are shown in Figure 4. The addition of elastomeric compatibilizer to pure PA6 does not significantly influence the storage moduli, as previously

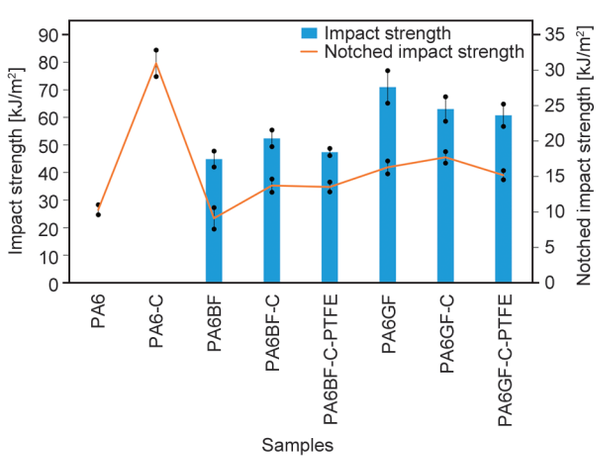

Figure 3. Impact and notched impact strength of materials.

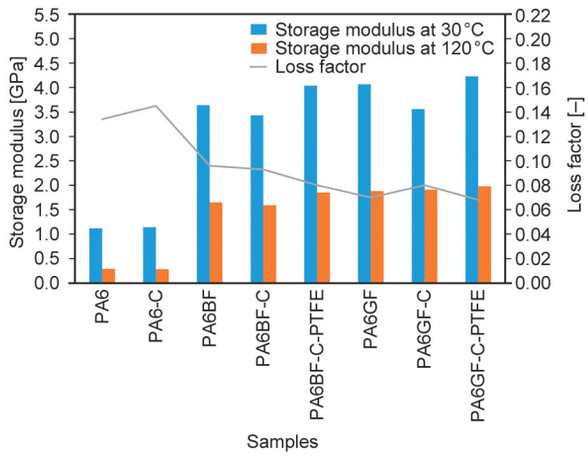

Figure 4. Storage moduli at 30, 120 °C, and loss factor determined by DMA.

noticed at tensile and flexural moduli. However, comparing reinforced specimens, compatibilised composites have the lowest moduli while lubricated composites have the highest moduli regardless of fiber type. Higher values are again obtained for GF-reinforced materials. The loss factor peak minimally increased with the introduction of compatibilizer and decreased with the introduction of reinforcement and PTFE, as presented in Figure 4, due to the hindrance of the matrix molecular mobility.

3.2. Thermal properties

Thermal properties determined by DSC are influenced by the addition of fibers. Both GF and BF act as nucleating agents and increase the degree of crystallinity (Table 2) from 30.1 to ≈33%. A further increase in fiber content in PA6, as explained below, reduced the crystallinity. This is most probably a consequence of steric hindrance. The polymer molecules are compressed between filler particles, which hinders their movement and thus the rate of crystallization, as already observed in other composites [19]. According to the results in Table 2, the

Table 2. DSC results of 1st cooling and 2nd heating.

	1. cooling		2. heating		
	T_c [°C]	ΔH_c [J/g]	T_m [°C]	ΔH_m [J/g]	X_c [%]
PA6	191.5	63.3	219.2	68.8	30.1
PA6C	192.0	64.2	220.2	69.1	31.1
PA6BF	191.6	49.1	220.5	53.8	33.7
PA6BF-C	190.9	50.7	220.5	49.3	32.2
PA6BF-PTFE-C	189.9	33.7	221.4	37.5	29.9
PA6GF	191.2	48.6	220.6	53.0	33.2
PA6GF-C	191.2	49.6	220.5	50.0	32.7
PA6GF-PTFE-C	190.2	32.8	220.9	40.1	32.0

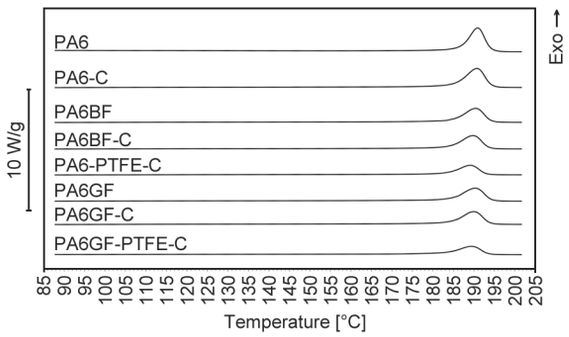

Figure 5. Normalized DSC curves of the cooling cycle.

steric hindrance is much more pronounced by BF. The effect can also be seen in Figure 5, which presents the DSC curves of the first cooling. The crystallization onset shifted to a lower temperature, and a broader peak was observed.

Thermal conductivity is an important factor in the application of gears. Good thermal conductivity reduces the temperature rise at the teeth and prolongs the lifetime of gears. Figure 7 shows the thermal conductivities of all materials. PA6 and PA6-C have a thermal conductivity in the range of 0.3 W/(m·K). With the addition of fibers, the thermal conductivity increases as would be expected for the addition of the component with the higher thermal conductivity. The increase is very similar (in the range of standard deviation) when comparing different fiber types. However, the addition of a compatibilizer slightly lowers the conductivity, while PTFE increases it, achieving a maximum of 0.39 W/(m·K) for PA6BF-PTFE-C. The latter results are a little surprising as the thermal conductivity of PTFE, according to various sources, is 0.26–0.30 W/(m·K). This can be explained by a higher concentration of fibers dispersed in PA6 in composites with PTFE. Although the nominal concentration of fibers is 30% in both cases, the PTFE is a particulate filler, so all the fibers are distributed within the smaller amount of PA6 (3 % in 52% PA6 instead of 30% in 70% PA6) (Table 1). A conductive path with a higher concentration of fibers in PA6 (36.6%) was formed around the PTFE particles, which increased the overall conductivity (Figure 6). Thermal conductivity of PA6/GF was calculated according to the Maxwell-Garnett model (Equation (2)):

$$\lambda_{com} = \lambda_m \frac{\lambda_f + 2\lambda_m + 2\phi(\lambda_f - \lambda_m)}{\lambda_f + 2\lambda_m - \phi(\lambda_f - \lambda_m)} \quad (2)$$

where λ_{com} – thermal conductivity of composite, λ_m – thermal conductivity of polymer matrix (PA6: 0.3 W/(m·K)), λ_f – thermal conductivity of filler (GF, average value 1.0), ϕ – volume fraction of filler

For 30 and 36% of GF samples, the thermal conductivities are 0.367 and 0.388 W/(m·K), respectively, which is in good agreement with observed results.

Figure 6. Schematic presentation of fiber concentration (30%) within (a) PA6 (red) and (b) after the addition of PTFE (blue).

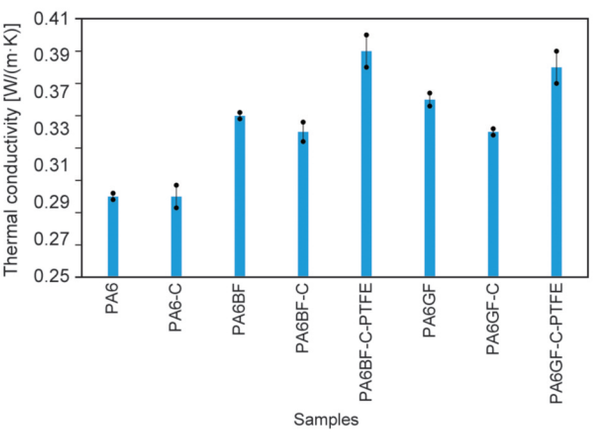

Figure 7. Thermal conductivity of materials.

3.3. Tribological properties

The tribological properties were investigated by the pin-on-disc method, and the results are shown in Figure 8. The addition of a compatibilizer increases the wear rate but slightly decreases the coefficient of friction compared to PA6. There appears to be a visible trend in the tribological performance of BF compared to GF. Mimaroglu *et al*. [20] also reported such a trend with Nanoclay and a compatibilizer compounded PA6/PP blend. This also becomes visible by comparing the tribological surface after testing (Figure 9). The running surface of the neat PA6 shows more glossy adhesive areas compared to PA6-C, which shows a much more homogenous surface structure, which acts as an indicator for lowering the CoF (Figures 9a and 9b). Furthermore, the increase in the wear rate becomes evident by comparing the counterbody surfaces, showing a more severe wear particle formation. However, the addition of fibers itself significantly reduces wear and also slightly lowers the coefficient of friction, which is

consistent with the general findings on the addition of GF [21].

The effect of the compatibilizer on the tribological properties of composites is different for GF and BF. A decrease in wear and friction coefficient was observed for PA6BF-C, while an increase in wear was observed for PA6GF-C compared to PA6BF and PA6GF, respectively. This could be linked to the different mechanical properties of BF and GF shown in Section 3.1. Based on the findings of Friedrich [22] in correlation with the tribological properties of polymeric compounds and the interaction of fibres with the polymeric matrix, in the recent paper, the BF seems to be softer than the GF, which leads to a less stiff gradient between matrix and filler So, in combination with the compatibilizer, a positive effect for BF and a negative effect for GF is noticeable. This could also be underpinned by comparing the running surface in Figures 9c, 9d and 9f, 9g. Figures 9c, 9d stays homogeneous, and Figures 9f, 9g shows a change, showing a rather inhomogeneous surface structure.

PTFE does not influence the coefficient of friction due to the dominating behaviour of fibre-counterpart interaction, which has an abrasive impact on the friction behaviour, but additionally reduces the wear rate. Optimal tribological performance, combining the lowest wear rate and the lowest coefficient of friction, was achieved with fiber reinforcement and internal lubrication with PTFE. These findings are in good correlation with the work of Li [23], showing that besides the stabilizing of the matrix with fibres, solid lubricants are needed to enhance the wear performance.

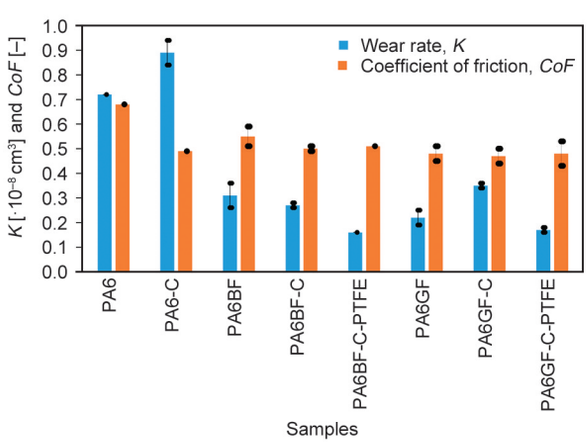

Figure 8. Wear rates and coefficients of friction as determined using the pin-on-disc method.

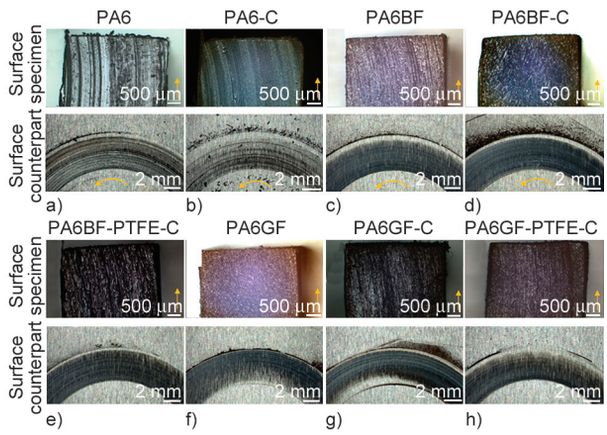

Figure 9. Light microscopic analysis of the sample running surfaces (50×) and the counterparts (7×) for all examined variants. Arrows indicate the moving direction. a) PA6, b) PA6-C, c) PA6BF, d) PA6BF-C, e) PA6BF-PTFE-C, f) PA6GF, g) PA6GF-C, h) PA6GF-PTFE-C.

3.4. Fiber length

Fiber length influences the mechanical properties of composites. Since both GF and BF are brittle, they break up into smaller pieces during the composite preparation and processing. To get a better insight into the fiber length and the influence of injection molding on it, we determined the fiber length distribution on the TGA residues of composite granulates and injection molded samples. The breakage of fibers is random, and a lot of particles smaller than the fiber thickness can be observed (5–10 µm). The length was calculated only for fibers with a length above 30 µm. Results are presented in Figure 10 and Table 3. Average fiber lengths were comparable and in the range of the standard deviation for all composites. Most of the fibers are on a length scale of 30–600 µm, although individual fibers of up to 2 mm can be found.

Table 3. Average fiber length before and after the injection molding.

	Fiber length [µm]	
	Before injection molding	**Injection moulded**
PA6BF	280±236	218±168
PA6BF-C	278±219	237±204
PA6BF-C-PTFE	240±186	281±194
PA6GF	312±198	267±153
PA6GF-C	234±181	210±148
PA6GF-C-PTFE	297±208	207±134

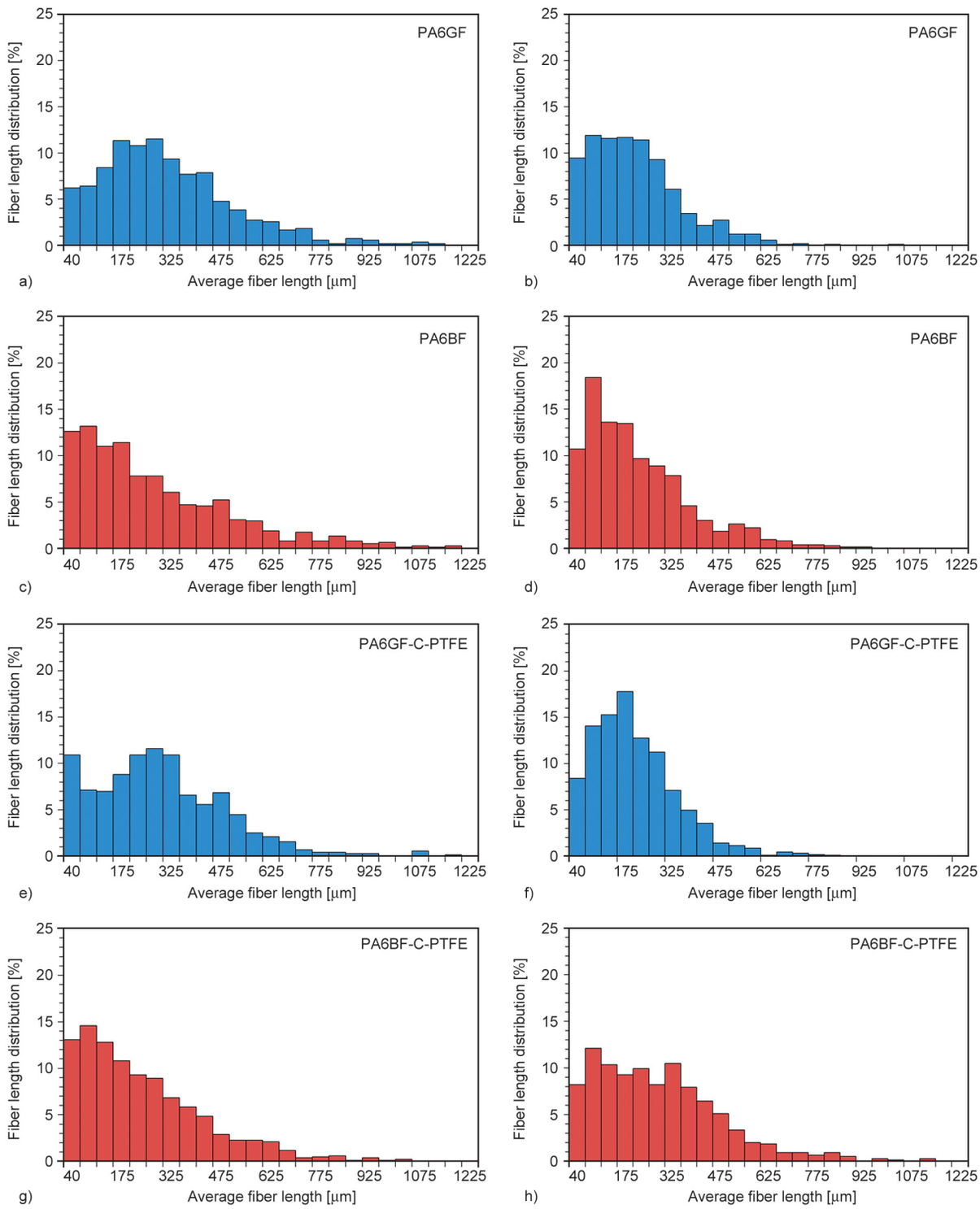

Figure 10. Fiber length distributions of reinforced materials after compounding (a), (c), (e), (g) and after the injection molding (b), (d), (f), (h).

3.5. SEM and EDS analysis of fracture surface

SEM and EDS analyses were performed to determine the differences in fracture mechanism and distribution of particles within the PA6 matrix. No significant differences were observed between the fractured surfaces of samples with GF or BF. The surfaces of PA6GF and PA6BF are shown as examples in Figure 11. The fibers are pulled out of the matrix due to the weak interfacial forces. An EDS mapping was performed to see the distribution of PTFE particles within the matrix since it is known that the PTFE is highly hydrophobic, while the fibers and PA6 are more hydrophilic. However, as also shown

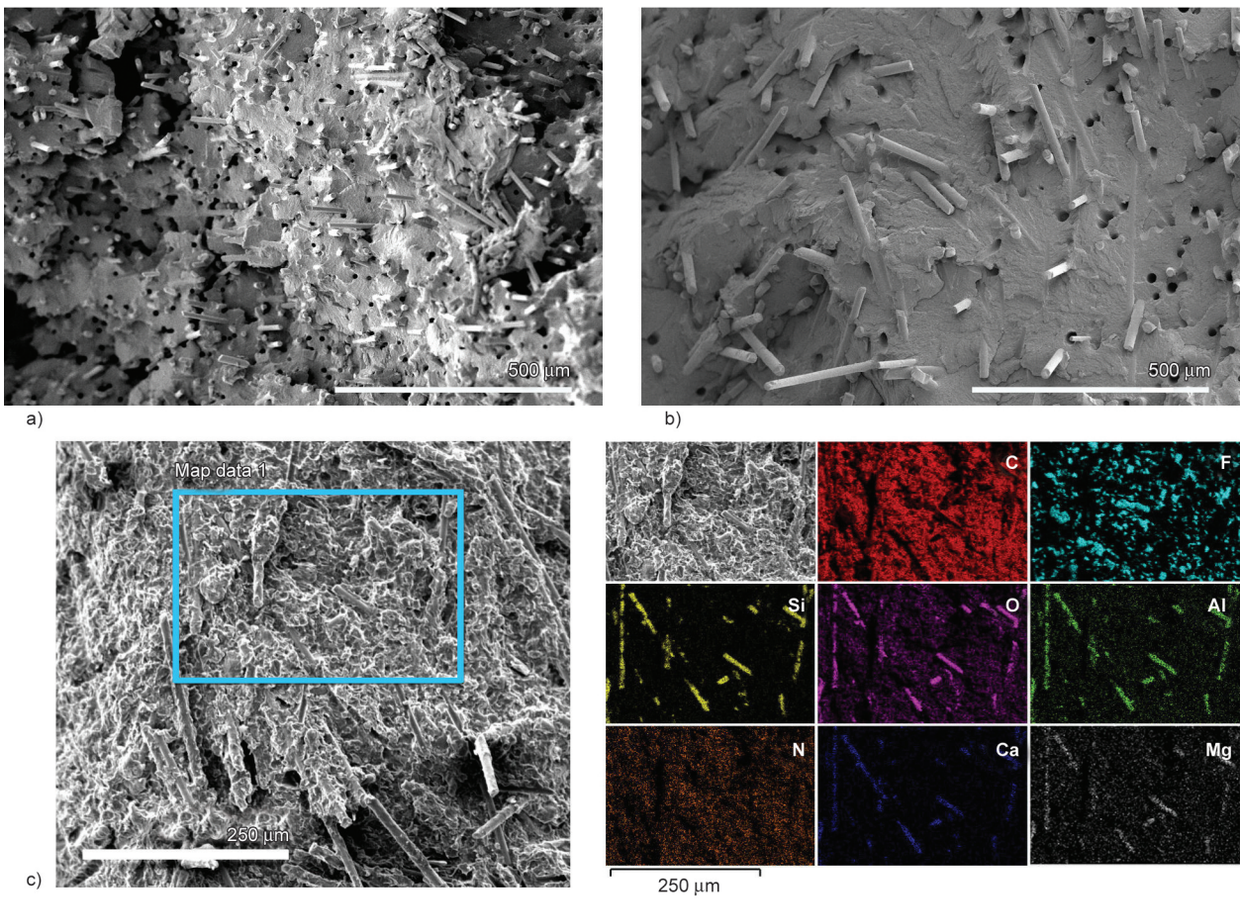

Figure 11. SEM images of the fracture surface of PA6GF (a) and PA6BF (b). SEM image of PA6GF C PTFE with corresponding EDS elemental maps of C, F, Si, O, Al, N, Ca, and Mg (c).

in Figure 11, the distribution of fluorine is very good. There were no particles larger than 50 µm observed, and most of them were smaller than 40 µm, which is the nominal size of the PTFE particles. It seems that during the mixing in the extruder, the fibers break into smaller and sharper particles, which cut PTFE particles into smaller fragments as well.

4. Conclusions

The goal of the present study was to compare the properties of composites of PA6 with GF and BF for gear applications. The composites were prepared under the same processing conditions to ensure the same history of the tested samples.

The mechanical properties of composites with GF are generally better than those of composites with BF. In both cases, the best mechanical properties were obtained with the addition of fibers and PTFE. Since PTFE does not possess high mechanical strength and is incompatible with PA6, this can be explained by the increased concentration of fibers within the PA6 matrix. The same is true for the highest thermal conductivity of composites with PTFE.

The mechanical properties of composites strongly depend on the fiber length; the longer the better. However, during the composite preparation in a twin-screw extruder, the fibers break into much smaller fibers and small particles. The average length of the fibers is reduced from 4–5 mm to several hundred micrometers. No important differences in length were observed between GF and BF. During injection molding, the most common technique for producing gears, additional fiber breakage occurs, although it is less extensive. The fiber length is further reduced by several tens of microns.

Both GF and BF slightly increased the crystallinity of PA6 and changed the size of the crystallites.

SEM and EDS mapping analyses showed that the interactions between the fibers (both GF and BF) and the PA6 matrix are not good. The fibers are pulled out of the matrix. However, despite large differences in surface tension between PA6 and PTFE, the distribution of PTFE particles in the PA6 matrix is very good. The PTFE particles are smaller than those specified by the manufacturer, likely due to the sharp GF or BF cutting of the particles during

the composite preparation process in the twin-screw extruder.

The tribological tests clearly show that fiber-based reinforcing materials have an influence on friction and wear behaviour. In addition to the use of compatibilizer and the use of solid lubricants such as PTFE, the potential for BF as a substitute for GF could be considered. Further investigations are still needed to adopt material formulations regarding the load collective for potential gear applications.

Acknowledgements

This work was carried out partly within the framework of the Incircular project, funded by the European Union's ERDF (Interregional Innovation Investments (I3) Instrument) grant agreement No 101114988 and partially through the SRIP – Future Factories initiative, partly funded by the European Regional Development Fund.

References

[1] Adesina A.: Performance of cementitious composites reinforced with chopped basalt fibres – An overview. Construction and Building Materials, **266**, 120970 (2021). https://doi.org/10.1016/j.conbuildmat.2020.120970

[2] Monaldo E., Nerilli F., Vairo G.: Basalt-based fiber-reinforced materials and structural applications in civil engineering. Composite Structures, **214**, 246–263 (2019). https://doi.org/10.1016/j.compstruct.2019.02.002

[3] Mohajerani A., Hui S-Q., Mirzababaei M., Arulrajah A., Horpibulsuk S., Abdul Kadir A., Rahman M. T., Maghool F.: Amazing types, properties, and applications of fibres in construction materials. Materials, **12**, 2513 (2019). https://doi.org/10.3390/ma12162513

[4] Fiore V., Scalici T., di Bella G., Valenza A.: A review on basalt fibre and its composites. Composites Part B: Engineering, **74**, 74–94 (2015). https://doi.org/10.1016/j.compositesb.2014.12.034

[5] Yang G., Park M., Park S-J.: Recent progresses of fabrication and characterization of fibers-reinforced composites: A review. Composites Communications, **14**, 34–42 (2019). https://doi.org/10.1016/j.coco.2019.05.004

[6] McConnell E. E., Kamstrup O., Musselman R., Hesterberg T. W., Chevalier J., Miiller W. C., Thevenaz P.: Chronic inhalation study of size-separated rock and slag wool insulation fibers in fischer 344/n rats. Inhalation Toxicology, **6**, 571–614 (1994). https://doi.org/10.3109/08958379409003042

[7] Kogan F. M., Nikitina O. V.: Solubility of chrysotile asbestos and basalt fibers in relation to their fibrogenic and carcinogenic action. Environmental Health Perspectives, **102**, 205 (1994). https://doi.org/10.2307/3432086

[8] Lund M. D., Yue Y-Z.: Influences of chemical aging on the surface morphology and crystallization behavior of basaltic glass fibers. Journal of Non-Crystalline Solids, **354**, 1151–1154 (2008). https://doi.org/10.1016/j.jnoncrysol.2006.11.031

[9] Ivanič A., Kravanja G., Kidess W., Rudolf R., Lubej S.: The influences of moisture on the mechanical, morphological and thermogravimetric properties of mineral wool made from basalt glass fibers. Materials, **13**, 2392 (2020). https://doi.org/10.3390/ma13102392

[10] Deák T., Czigány T., Tamás P., Németh Cs.: Enhancement of interfacial properties of basalt fiber reinforced nylon 6 matrix composites with silane coupling agents. Express Polymer Letters, **4**, 590–598 (2010). https://doi.org/10.3144/expresspolymlett.2010.74

[11] Khandelwal S., Rhee K. Y.: Recent advances in basalt-fiber-reinforced composites: Tailoring the fiber-matrix interface. Composites Part B: Engineering, **192**, 108011 (2020). https://doi.org/10.1016/j.compositesb.2020.108011

[12] Jamshaid H., Mishra R.: A green material from rock: Basalt fiber – A review. Journal of the Textile Institute, **107**, 923–937 (2016). https://doi.org/10.1080/00405000.2015.1071940

[13] Dorigato A., Pegoretti A.: Fatigue resistance of basalt fibers-reinforced laminates. Journal of Composite Materials, **46**, 1773–1785 (2012). https://doi.org/10.1177/0021998311425620

[14] Lopresto V., Leone C., de Iorio I.: Mechanical characterisation of basalt fibre reinforced plastic. Composites Part B: Engineering, **42**, 717–723 (2011). https://doi.org/10.1016/j.compositesb.2011.01.030

[15] Asadi A., Baaij F., Mainka H., Rademacher M., Thompson J., Kalaitzidou K.: Basalt fibers as a sustainable and cost-effective alternative to glass fibers in sheet molding compound (SMC). Composites Part B: Engineering, **123**, 210–218 (2017). https://doi.org/10.1016/j.compositesb.2017.05.017

[16] Elmahdy A., Verleysen P.: Mechanical behavior of basalt and glass textile composites at high strain rates: A comparison. Polymer Testing, **81**, 106224 (2020). https://doi.org/10.1016/j.polymertesting.2019.106224

[17] Carmisciano S., de Rosa I. M., Sarasin F., Tamburrano A., Valente M.: Basalt woven fiber reinforced vinylester composites: Flexural and electrical properties. Materials & Design, **32**, 337–342 (2011). https://doi.org/10.1016/j.matdes.2010.06.042

[18] Zhao R-G., Luo W-B., Xiao H-M., Wu G-Z.: Water-absorptivity and mechanical behaviors of PTFE/PA6 and PTFE/PA66 blends. Transactions of Nonferrous Metals Society of China, **16**, s498–s503 (2006). https://doi.org/10.1016/S1003-6326(06)60243-4

[19] Oseli A., Vesel A., Mozetič M., Žagar E., Huskić M., Slemenik Perše L.: Nano-mesh superstructure in single-walled carbon nanotube/polyethylene nanocomposites, and its impact on rheological, thermal and mechanical properties. Composites Part A: Applied Science and Manufacturing, **136**, 105972 (2020). https://doi.org/10.1016/j.compositesa.2020.105972

[20] Mimaroglu A., Unal H., Yetgin S. H.: Tribological properties of nanoclay reinforced polyamide-6/polypropylene blend. Macromolecular Symposia, **379**, 1700022 (2018). https://doi.org/10.1002/masy.201700022

[21] Gyurova A. L., Schlarb A. K.: State-of-the-art: On the action of various reinforcing fillers and additives for improving the sliding friction and wear performance of polymer composites. Part 1: Short fibers, internal lubricants, particulate fillers. Journal of Plastics Technology, **4**, 1–31 (2008).

[22] Friedrich K.: Wear of reinforced polymers by different abrasive counterparts. in 'Friction and wear of polymer composites' (ed.: Friedrich K.) Elsevier, Amsterdam, 233–287 (1986). https://doi.org/10.1016/B978-0-444-42524-9.50012-0

[23] Li J.: The effect of PTFE on the mechanical and friction and wear properties of GF/PA6 composites. Advanced Materials Research, **284–286**, 2370–2373 (2011). https://doi.org/10.4028/www.scientific.net/amr.284-286.2370